Journal of Hazardous Materials 170 (2009) 895–901

Contents lists available at ScienceDirect

Journal of Hazardous Materials

journal homepage: www.elsevier.com/locate/jhazmat

Reductive dechlorination of hexachlorobenzene by Cu/Fe bimetal in the presence of nonionic surfactant

Zhonghua Zheng[a], Songhu Yuan[a,b,*], Yang Liu[a], Xiaohua Lu[a], Jinzhong Wan[a], Xiaohui Wu[a], Jing Chen[a]

[a] Environmental Science Research Institute, Huazhong University of Science and Technology, Wuhan 430074, PR China
[b] State Key Laboratory of Soil and Sustainable Agriculture, Institute of Soil Science, Chinese Academy of Sciences, Nanjing 210008, China

ARTICLE INFO

Article history:
Received 25 February 2009
Received in revised form 11 May 2009
Accepted 11 May 2009
Available online 19 May 2009

Keywords:
Zero-valent iron
Hexachlorobenzene
Dechlorination
Surfactants

ABSTRACT

This study investigated the enhancement of nonionic surfactant (TritonX-100, TX-100) on the reductive dechlorination of hexachlorobenzene (HCB) by microscale Cu/Fe bimetal. HCB reduction by Cu/Fe without TX-100, in aqueous TX-100, adsorbed with TX-100 and prepared with TX-100 was compared. Results showed that HCB reduction by Cu/Fe in aqueous TX-100 increased with increasing TX-100 concentration, reached a maximum of 98.6% when aqueous TX-100 concentration attained its critical micelle concentration (CMC), and decreased with the further increase in TX-100 concentration. The mechanism was suggested as the increased HCB mass transport at low TX-100 concentration below CMC and the coverage of reactive sites at high TX-100 concentration above CMC. The greatest reduction was achieved by Cu/Fe in the presence of 0.2 mM TX-100, followed by Cu/Fe adsorbed and prepared with 0.2 mM TX-100. Pentachlorobenzene and tetrachlorobenzene were found as the main dechlorination intermediates. Successive reduction by Cu/Fe in aqueous TX-100 solution could be maintained above 98% for four cycles. It is an alternative to use nonionic surfactants to enhance the reductive dechlorination of hydrophobic polychlorinated aromatic hydrocarbons (PCAH) by Cu/Fe bimetal.

1. Introduction

Polychlorinated aromatic hydrocarbons (PCAH), such as polychlorinated biphenyls (PCBs) and hexachlorobenzene (HCB), have attracted global attention because of their high toxicity, extensive existence and long-term persistence [1,2]. The Superfund of USA has identified and treated many PCAH contaminated waters and sediments [3]. A previous work has found a highly HCB contaminated site in central China [4]. The biodegradation of PCAH is rather difficult due to their high stability and toxicity. In general, the toxicity of PCAH decreases with the decrease of chlorine substitution, and thus the biodegradability is increased. So, reductive dechlorination provides an alternative approach to the treatment of PCAH prior to biodegradation.

Zero-valent iron (ZVI) has been proven to be promising for the reductive dechlorination of chlorinated hydrocarbons [5–7]. However, the dechlorination of PCAH becomes very slow, or even no significant dechlorination was observed for a long time [8,9]. Researchers have developed bimetals and nanoscale ZVI to increase the dechlorination. In particular, palladized microscale and nanoscale iron were found to reach rapid and even complete dechlorination of PCBs [9–12]. The increased dechlorination of HCB by Ag/Fe was also reported [8]. However, the modification with Pd or Ag dramatically increases cost. It is therefore desirable to find economical and effective methods for the modification.

The reduction of pollutants by ZVI generally involves the mass transport of pollutants from aqueous solution to ZVI surface and the subsequent surface reduction [13]. Most literatures are focused on the promotion of surface reduction by ZVI modification with noble metals. The generally used metals include Pd, Ni, Pt, and Cu [6], among which Cu is the cheapest one. In contrast, limited work has been done regarding the mediation of mass transport process. Nevertheless, mass transport greatly influences the reduction, particularly for hydrophobic compounds like PCAH.

Surfactants have amphiphilic structure, containing a polar hydrophilic moiety and a nonpolar hydrophobic moiety. Surfactants can be adsorbed at interfaces and reduce interfacial energies. So, surfactants can be used to mediate the mass transport in dechlorination process. Sayles et al. [14] noted that the dechlorination of DDT by ZVI was significantly enhanced in the presence of TritonX-114. Several studies have showed enhanced reduction by cationic surfactants [15–18]. Cho and Park [19] reported that nonionic and cationic surfactants increased but anionic surfactant decreased tetrachloroethene (PCE) dechlorination by ZVI. Very recently, Zhu et al. [20] proposed surfactants inhibited the access of hydrophobic substrate to the surface reactive sites by partitioning the substrate into its hydrophobic interiors at high concentration above critical micelle concentration (CMC), and attributed to dechlorination by

* Corresponding author. Tel.: +86 27 87792159; fax: +86 27 87792159.
E-mail address: yuansonghu622@hotmail.com (S. Yuan).

0304-3894/$ – see front matter © 2009 Elsevier B.V. All rights reserved.
doi:10.1016/j.jhazmat.2009.05.052

promoting the partitioning of hydrophobic substrate on the interfacial film at low concentration below CMC. However, the influence of surfactant on PCAH dechlorination by microscale bimetal, particularly cheap bimetals like Cu/Fe, has been seldom investigated [20].

In this study, a relatively cheap metal of Cu was used as the second metal to prepare Cu/Fe bimetal. HCB and TritonX-100 (TX-100) were selected as representative PCAH and surfactants, respectively. The reductive dechlorination of HCB by Cu/Fe in the presence of TX-100 and by Cu/Fe modified with TX-100 was compared. The objectives are to investigate the influence of TX-100 on the reductive dechlorination of HCB by Cu/Fe, and to provide more information on surfactant-mediated dechlorination by bimetals.

2. Experimental

2.1. Chemicals

HCB (99.0%) was purchased from Shanghai General Reagent Factory, China. TX-100 (analytical purity, 99.0%) was from Amresco 94. Pentachlorobenzene (PeCB, 98%), 1,2,4,5-tetrachlorobenzene (1,2,4,5-TeCB, 99%), 1,2,3,4-tetrachlorobenzene (1,2,3,4-TeCB, 99%), 1,2,3-trichlorobenzene (1,2,3-TCB, 99%), 1,2,4-trichlorobenzene (1,2,4-TCB, 99%), 1,3,5-trichlorobenzene (1,3,5-TCB, 99%), 1,2-dichlorobenzene (1,2-DCB, 99%) and 1,3-dichlorobenzene (1,3-DCB, 98%) were from Sigma–Aldrich, and 1,2,3,5-tetrachlorobenzene was from Fluka. Iron particles (99%) were from Tianjin Kermel Chemical Reagent Development Center with particle size less than 100 mesh (0.15 mm). $CuCl_2{\cdot}2H_2O$ (analytical purity, 99.0%) was from Chengdu Chemical Reagent Factory, China. Deionized water was used for the preparation of solutions. All the other reagents used were above analytical grade.

2.2. Procedures

All the reduction and adsorption experiments were carried out in 11-mL glass vials sealed with Teflon screw caps. The reduction by four types of iron reductants, iron particles, Cu/Fe, Cu/Fe adsorbed with TX-100, and Cu/Fe prepared with TX-100, was compared. A mass of 0.2 g of iron particles was washed with 0.8 mL of HCl (1 M) for 30 min, and purged with deionized water to neutral (termed Fe particles). The acid-washed iron was mixed with 5 mL of $CuCl_2$ solution (32 mM) for 60 min, and washed with deionized water to neutral (termed Cu/Fe). Assuming the complete reduction [6,21], 5% loading of Cu on Fe was achieved. The complete reduction was also confirmed by the disappearance of blue color of $CuCl_2$ solution. The prepared Cu/Fe was further equilibrated with 5 mL of TX-100 solution (0.2 mM) (termed Cu/Fe in aqueous) for 60 min (120 rpm, $25 \pm 2\,^{\circ}C$). Cu/Fe adsorbed with TX-100 was obtained by centrifugation and pouring out the aqueous solution (termed Cu/Fe adsorbed). For Cu/Fe prepared with TX-100, the acid-washed iron was mixed with 5 mL of $CuCl_2$ solution (32 mM) containing 0.2 mM TX-100 (termed Cu/Fe prepared). Upon the completion of reductant preparation, 5 mL of HCB solution (0.2 mg L^{-1} with 0.1% acetone) with or without TX-100 was added. The aqueous pH was kept at 3.0 by 0.5 M acetic buffer. The surrounding temperature was $25 \pm 2\,^{\circ}C$. Each run was performed at least in triplicate. No attempt was used to purge O_2 contained in the solution and vial.

For the adsorption of TX-100 on iron reductants, the freshly prepared Cu/Fe was equilibrated with 5 mL of different concentrations of TX-100 solution in the vials (120 rpm, $25 \pm 2\,^{\circ}C$). The adsorbed TX-100 was obtained from the difference of initial and equilibrated concentration. Regarding the desorption of TX-100 from reductants, Cu/Fe adsorbed or prepared with TX-100 was equilibrated with deionized water. The aqueous concentration of TX-100 at different time intervals was determined to evaluate the desorption. Each run was performed at least in triplicate.

2.3. Analysis

At regular time intervals of reduction experiments, the vials were sacrificed to analyze the concentration of HCB and dechlorination intermediates. Three mL of hexane was added to the vial to extract all HCB and dechlorination intermediates [4] The supernatant was filtered with 0.45 μm filtration membrane. HCB and dechlorination intermediates in the filtrate were analyzed by a Hewlett-Packard 6890 GC equipped with an electron capture detector (ECD) and a ZB-5 capillary column (Phenomenex, USA). The oven was heated from 160 to 240 °C at a rate of 10 °C min^{-1}, held for 2 min. The flow rate of carrier gas (nitrogen 99.999%) was 1.5 mL min^{-1}. The injector and detector temperatures were 250 and 300 °C, respectively. The split ratio was 2 and injection volume was 1 μL. The recovery of HCB in the extraction was proved to be above 90%.

The surface tension of TX-100 was determined by a tensiometer (JK99B Automatic tensiometer, Shanghai Zhongchen Digital Technology Equipment Ltd., China), and the CMC was obtained as 0.11 mM from the inflection of the plot of surface tension versus logarithm surfactant concentration (data not shown). TX-100 was measured by an HPLC system (Aligent) with a reverse-phase Cosmosil 5C18-MS-II column (250 mm × 4.6 mm I.D., 5 μm). Prior to analysis, a droplet of high concentration of Na_2EDTA was added to avoid the interference of ferrous iron. The mobile phase was a mixture of methanol and 0.5% acetic acid aqueous solution with volume ratio of 80:20 at the flow rate of 1 mL min^{-1}. The wavelength was set at 225 nm. The volume of injection was 20 μL. Calibration curves were drawn for the quantitative analysis. The correlation coefficients (R^2) of the fitted line were above 0.990.

The prepared reductants were separated by centrifugation and air-dried prior to characterization. Surface area determined by sorption of N_2 at 77 K (Micromeritics ASAP2020) using Brunauer–Emmett–Teller adsorption indicates 2.21 $m^2\,g^{-1}$ for the Cu/Fe prepared. Scanning electron microscopy (SEM) and energy dispersive X-ray (EDX) analysis were performed on a FEI Quanta 200 scanning electron microscope. X-ray powder diffraction (XRD) patterns were obtained on a PANalytical B. V. X'Pert PRO X-ray diffractometer with CuK radiation.

3. Results and discussion

3.1. Characterization of reduction particles

Fig. 1 shows the XRD patterns of acid-washed Fe and prepared Cu/Fe bimetals. For the XRD patterns of Fe particles, the peaks at 45.1° and 65.0° can be indexed to the (1 1 0) and (2 0 0) planes of cubic α-Fe^0 [20,22]. No Fe oxide peaks were measured, indicating that acid-wash can mostly remove the oxides in Fe particles. The XRD patterns for Cu/Fe clearly suggest the loading of Cu^0 on Fe surface. Likewise, Cu oxides were not detected. This is consistent with the literatures [21,23], where Cu^0 was confirmed as the sole Cu on Fe surface by X-ray photoelectron spectroscopy analysis. When Cu/Fe was adsorbed with TX-100, the peaks for Cu were somewhat reduced. Regarding Cu/Fe prepared with TX-100, the peaks for both Cu and Fe were reduced, and the peak for Cu at 51.0° almost disappeared. When 0.2 mM TX-100 was present in Cu/Fe preparation process, Fe surface was covered with a thin layer of adsorbed TX-100 [24], which lowered the reduction of Cu^{2+} on Fe surface and impeded the interaction between produced Cu^0 and Fe surface. Thus, the decreased Cu loading can be expected for Cu/Fe prepared with TX-100.From the SEM images in Fig. 2, Fe particles after acid-wash gave a relatively smooth surface embedded with

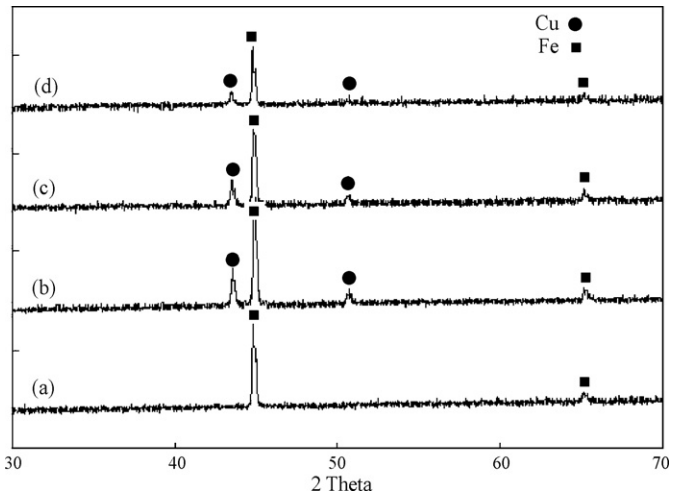

Fig. 1. XRD patterns of (a) acid-washed Fe particles, (b) Cu/Fe, (c) Cu/Fe adsorbed with TX-100 and (d) Cu/Fe prepared with TX-100.

erosion holes. The corresponding EDX analysis (Table 1) implies the presence of small quantities of Fe oxide on the surface. After deposition of Cu, the surface became coarse and was scattered with many microscale particles. From the EDX analysis of the region scattered with particle, we may deduce that the microscale particles were ascribed to the loading of Cu^0. Similar particle scattered images were also observed by Liou et al. [25]. However, when Cu/Fe was prepared with 0.2 mM TX-100, smooth, flossy and particle scattered images were observed on the surface. We ascribed the smooth surface to the coverage of TX-100, which inhibited Fe corrosion and Cu loading. The spot EDX analysis of the flossy surface shows the presence of high O content and low Cu content (6.26%). As no crystalline Fe or Cu oxides were identified from XRD patterns, we assume the high O content was originated from the growth of amorphous Fe oxides.

3.2. Adsorption and desorption of TX-100 on Cu/Fe

The time profiles of TX-100 adsorption on Cu/Fe in Fig. 3a show that the adsorption equilibrium was quickly achieved within 30 min. It was also addressed that the complete sorption of humic acid on nanoscale ZVI was achieved less than 20 min [26]. From the adsorption isotherm in Fig. 3b, it can be seen that the adsorbed TX-100 on Cu/Fe increased with the increase in aqueous TX-100 concentration. Regression results show that the sorption process was satisfactorily fitted by linearity ($C_s = 6.72C_e + 0.07$, $R^2 = 0.947$), followed by Freundlich ($C_s = 6.17C_e^{0.67}$, $R^2 = 0.910$), and could not be well expressed by Langmuir ($C_e/C_s = 0.05C_e + 0.10$, $R^2 = 0.282$). Generally, iron surface contains hydrophobic graphite inclusions, which is mainly responsible for the adsorption of hydrophobic organic compounds (HOCs) [27]. The presence of carbon was also revealed in Cu/Fe from SEM-EDX (Table 1), which resulted in the high affinity of TX-100 to Cu/Fe surface. It is also noted that a good linearity between the aqueous and initial TX-100 concentration (C_i) was obtained ($C_e = 0.79C_i$, $R^2 = 0.998$). The sorption isotherm is in agreement to the sorption of TX-100 on Fisher cast Fe particles reported by Loraine [16], but different from Langmuir sorption isotherm obtained by Cho and Park [19].

Negligible TX-100 desorption (below detection limit) was measured for Cu/Fe adsorbed and prepared with Cu/Fe. This indicates

Table 1
Element content from SEM/EDX analysis.

Element fraction	Fe	Cu/Fe	Cu/Fe prepared
CK (%)	6.63	4.71	6.83
OK (%)	2.39	2.40	16.39
Au (%)	5.38	6.04	5.01
FeK (%)	86.60	28.08	65.11
CuK (%)	0	58.82	6.26

Note: the values were corresponding to Fig. 2.

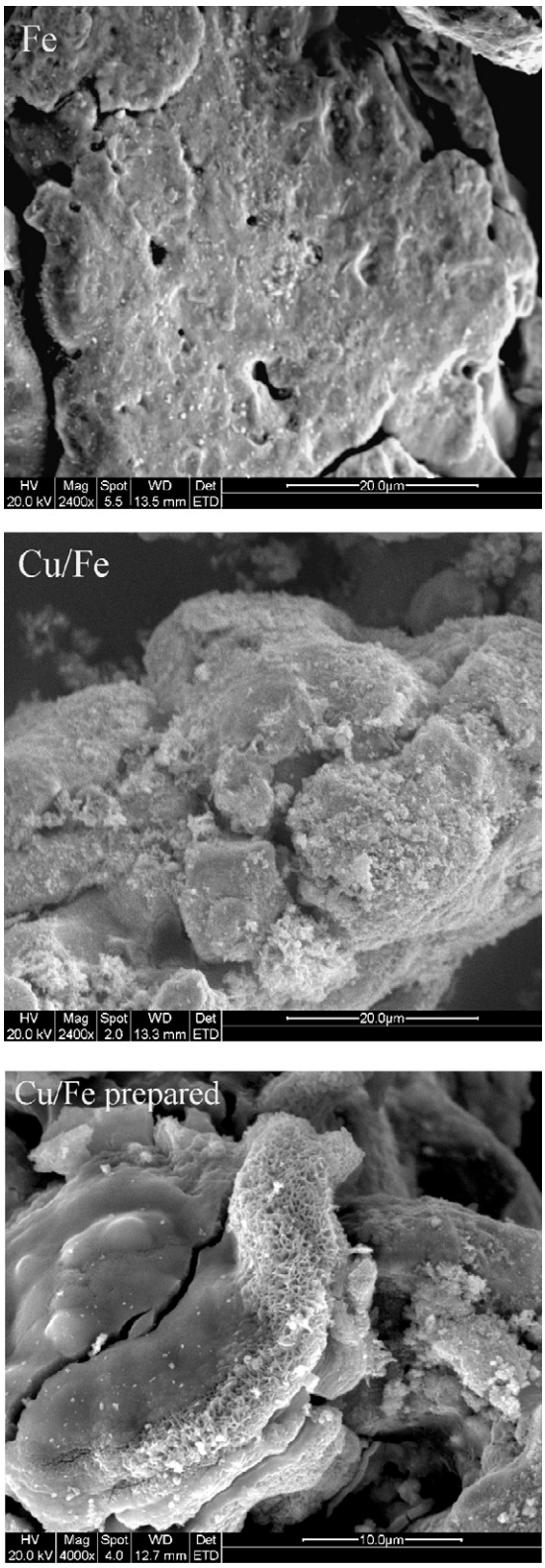

Fig. 2. SEM image of Fe, Cu/Fe and Cu/Fe prepared with TX-100.

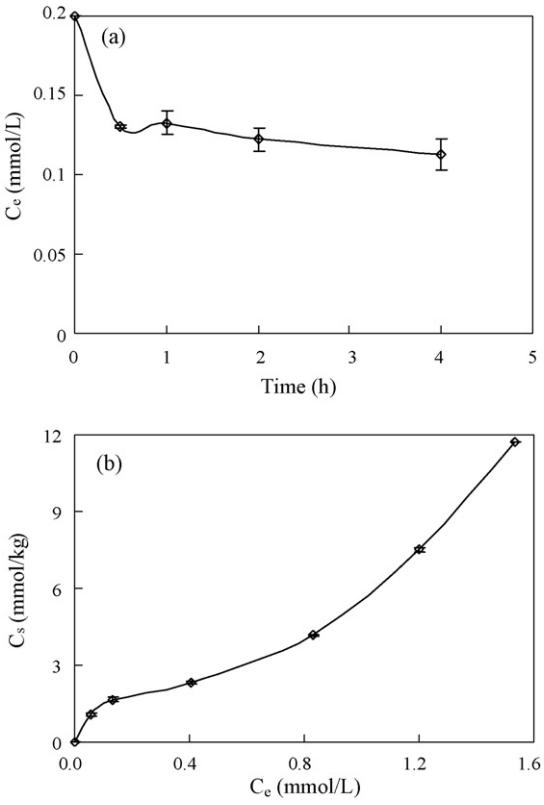

Fig. 3. (a) Variation of aqueous TX-100 with time in sorption process, $C_{TX\text{-}100}$ = 0.2 mM; (b) sorption isotherm of TX-100 on Cu/Fe. C_e and C_s refer to the equilibrium aqueous and solution concentration, respectively.

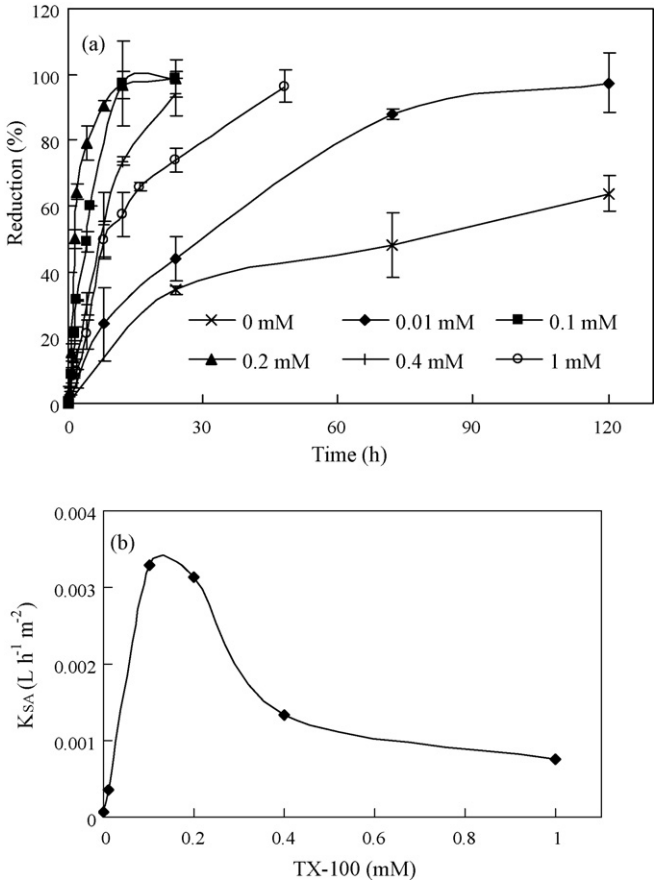

Fig. 4. (a) Influence of TX-100 concentration on HCB reduction; (b) variation of surface area-normalized pseudo-first-order kinetic rate constants with TX-100 concentration.

that the adsorbed TX-100 was strongly bounded to Cu/Fe surface, which is similar to the desorption of cationic surfactants adsorbed on Fe particles [15,17]. So, regarding the reduction of HCB by Cu/Fe adsorbed and prepared with TX-100 in the following sections, the influence of TX-100 release on reduction can be excluded.

3.3. Reduction of HCB by Cu/Fe in the presence of TX-100

The reduction of HCB by Cu/Fe with different concentrations of TX-100 is shown in Fig. 4. Control experiments show less than 20% reduction of HCB by acid-wash iron particles in the presence and absence of TX-100 within 15 d. Xu and Zhang [8] also reported negligible reduction of HCB by Aldrich Fe particles. Fig. 4a shows that significant HCB reduction was achieved by Cu/Fe in the absence of TX-100 (0 mM), and 63.8% of HCB was reduced for 120 h treatment. It is encouraging that near complete reduction of HCB was attained by Cu/Fe in the presence of TX-100. Furthermore, the reduction rates increased with the increase in TX-100 concentration less than 0.2 mM, and decreased with the further increase in TX-100 concentration to 1 mM, but still higher than that in the absence of TX-100.

In the reduction with TX-100, both aqueous and adsorbed surfactants existed. The aqueous surfactants, including monomer and micelle, attributed to the dissolution and desorption of HCB, while the adsorbed surfactants on reactive and nonreactive sites benefited the sorption of HCB. It has been obtained above that the adsorbed TX-100 increased linearly with the increase in initial TX-100 concentration. At TX-100 concentration lower than 0.2 mM, the aqueous TX-100 was less than or approximately equal to CMC, which could not attribute to the dissolution and desorption of HCB. The adsorbed TX-100 was preferentially bound to nonreactive sites such as graphite inclusions [16,27], which decreased the adsorption of HCB to nonreactive sites and increased the adsorption of HCB to Cu/Fe surface via hydrophobic interaction between adsorbed TX-100 and HCB. Hence, the transport of HCB from solutions to Cu/Fe surface, particularly reactive sites, and the reduction rates were facilitated. However, at high TX-100 concentration above 0.2 mM, the adsorbed TX-100 may further cover the reactive sites and impede the surface reaction, and the micelles in aqueous solution inhibited the sorption of HCB due to the increased solubilization and desorption. As a result, the decline of reduction rates at high concentration was obtained. Zhu et al. [20] also concluded that surfactants at concentration below CMC benefited trichlorobenzene dechlorination, and at high concentration above CMC inhibited dechlorination by partitioning the substrate into its hydrophobic interiors. Loraine [16] reported similar results for PCE dechlorination, but found an inhibition of trichloroethene (TCE) dechlorination in the presence of TX-100. It is concluded that the enhancement with surfactants increased with the increase in substrate hydrophobicity [16].

The surface area-normalized pseudo-first-order kinetic rate constants were calculated to give a straightforward comparison with the literatures. The influence of TX-100 concentration on HCB reduction is also clearly reflected in Fig. 4b. The rate constants for HCB reduction herein were about 100-fold higher of HCB reduction with ZVI alone reported by Lu et al. [28], and much lower than trichlorobenzene dechlorination with Pd/Fe supported on silicon and chitosan [29]. The reduction rate herein is also much faster than the reduction of HCB by nanoscale ZVI and nanoscale Pd/Fe (the maximal reduction efficiency was less than 70%) [30].

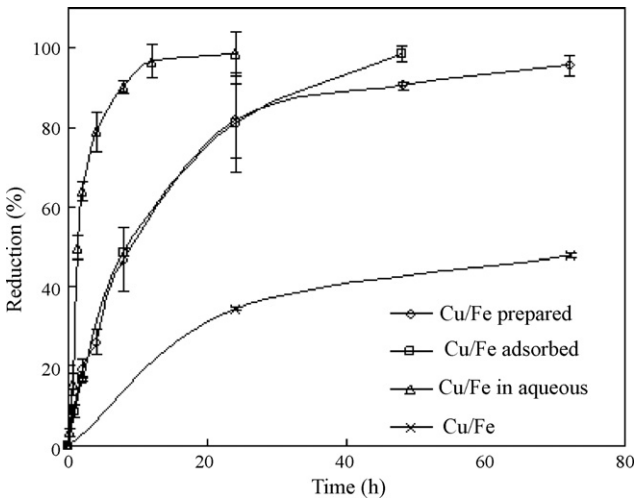

Fig. 5. Reduction of HCB by different Cu/Fe reductants.

3.4. Comparison of HCB reduction by different Cu/Fe reductants

In order to reveal the influence of TX-100 on HCB reduction, we compared the reduction of HCB by different Cu/Fe reductants (Fig. 5). The concentration of TX-100 was 0.2 mM. The fastest reduction was achieved by Cu/Fe in aqueous TX-100, followed by Cu/Fe adsorbed and prepared with TX-100, and the slowest reduction without TX-100. The different reduction can be explained from the contribution of mass transport and surface reduction. In the absence of TX-100, the mass transport of HCB was the slow and most adsorption appeared on the hydrophobic nonreactive sites [27], but the surface reduction was assumed to be fast due to the absolute exposure of reactive sites. The slowest reduction without TX-100 suggests that mass transport and adsorption on reactive sites mainly determined HCB reduction. Cu/Fe adsorbed with TX-100 had almost identical TX-100 loading with Cu/Fe prepared with TX-100, so very similar reduction profiles were obtained. As suggested in Section 3.3, the facilitated mass transport of HCB to Cu/Fe surface, particularly reactive sites, was responsible for the faster reduction in the presence of TX-100. The slower reduction at later stage for Cu/Fe prepared with TX-100 than for Cu/Fe adsorbed with TX-100 was probably resulted from its slower surface reduction. The XRD patterns (Fig. 1) show weaker peaks of Cu with TX-100 than without TX-100, and SEM-EDX reveals much lower fraction of Cu in Cu/Fe prepared with TX-100 than Cu/Fe alone. It is known that the reduction of contaminant by bimetals happened on the second metal and greatly depended on the loading of the second metal [6,10,20]. Besides, the presence of TX-100 impeded electron transfer from Fe to Cu through the interface in Cu/Fe prepared with TX-100. So, it is reasonable for the slower reduction by Cu/Fe prepared with TX-100. The faster reduction by Cu/Fe in aqueous TX-100 than by Cu/Fe adsorbed with TX-100 further suggests that mass transport mainly contributed to the reduction, because the same Cu/Fe particles and variables were used except the presence of aqueous TX-100. In reduction process, Cu/Fe surface became rugged by iron corrosion, which made more new surface sites exposed to solution. The presence of aqueous TX-100 may be further adsorbed onto these sites and contributed to the mass transport. The results obtained here are quite different from the literatures [15,17], where ZVI adsorbed with cationic surfactants showed better performance compared with ZVI immersed in aqueous cationic surfactant solutions. The difference may be due to the different characteristics and sorption behavior of nonionic and cationic surfactants.

3.5. Dechlorination intermediates of HCB reduction by different Cu/Fe reductants

The reduction of HCB by different Cu/Fe reductants was further compared from the production of dechlorination intermediates.

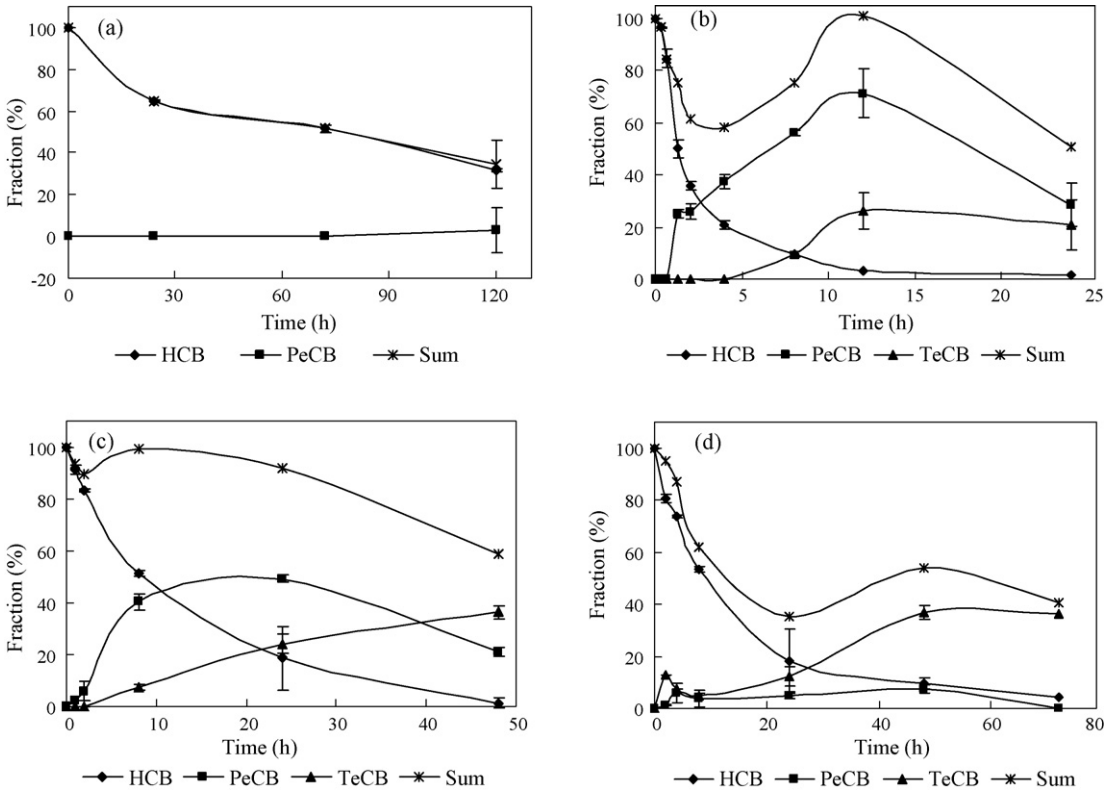

Fig. 6. Comparison of HCB dechlorination intermediates by (a) Cu/Fe, (b) Cu/Fe in aqueous TX-100, (c) Cu/Fe adsorbed with TX-100 and (d) Cu/Fe prepared with TX-100.

Fig. 6a shows that only low fraction of PeCB (<3%) was produced after 72 h. The concentration of TX-100 was 0.2 mM. In the reduction of HCB by Fe alone under the same conditions, above 80% recovery of HCB was measured, indicating that HCB could be mostly extracted in iron corrosion process. So, it can be suggested that HCB reduction by Cu/Fe without TX-100 led to the production of less chlorinated benzenes (such as less than 3 chlorine) or even benzene. Because the GC signals of these intermediates at ECD were much weaker compared to chlorobenzenes with more chlorine substituents (such as more than 3 chlorine), and the initial HCB concentration was very low (0.2 mg L^{-1}), less than three chlorinated benzenes could not be quantified in this study. The dechlorination selectivity of chlorinated benzenes by Cu/Fe in the presence of different surfactants is currently under investigation in our laboratory.

Regarding the reduction by Cu/Fe in aqueous TX-100 for 24 h (Fig. 6b), PeCB fraction increased to 71% in initial 12 h and decreased in later stage, and TeCB was measured after 4 h reduction. It is unexpected that a valley of the sum fraction appeared at around 4 h. Since above 80% recovery of HCB was confirmed in the reduction by Fe alone in aqueous TX-100, the valley sum was assumed to be resulted from the incomplete extraction with Cu/Fe coated with oxides and the produce of less chlorinated benzenes. The accumulation of PeCB in initial stage implied that PeCB dechlorination under this condition was difficult or very slow. It is noted that PeCB fraction decreased after 12 h while TeCB fraction was unchanged, which indicated the production of less chlorinated benzenes. In the reduction of HCB (4 mg L^{-1}) by Ag/Fe subcolloidal particles, Xu and Zhang [8] revealed that 75% dechlorination intermediates were presented as trichlorobenzenes and tetrachlorobenzenes, and PeCB fraction was negligible. Shih et al. [30] obtained less than 50% recovery of chlorobenzenes in the dechlorination of HCB by nanoscale ZVI and nanoscale Pd/Fe, and TCB was identified as the main intermediates.

In the reduction by Cu/Fe adsorbed with TX-100 for 48 h, similar profiles of HCB and dechlorination intermediates were observed except the continuous increase in TeCB fraction (Fig. 6c). However, in the reduction by Cu/Fe prepared with TX-100 (Fig. 6d), TeCB was accumulated much more than PeCB, and the sum was reduced more largely. This implied that HCB dechlorination by Cu/Fe prepared with TX-100 was different from that by Cu/Fe in aqueous TX-100 and adsorbed with TX-100. The different surface properties were accountable for the different mechanism. As found in Section 3.1, the Cu content was much less in Cu/Fe prepared with TX-100 than without TX-100 (Figs. 1 and 2), and the surface image of Cu/Fe prepared with TX-100 was different from that of Cu/Fe prepared without TX-100 (Fig. 2). The different surface properties may lead to different selectivity to different chlorinated benzenes [15,17]. In addition, Fe surface was pre-covered with TX-100 in the preparation process, the electron transfer through Cu–Fe interface was more difficult compared with Cu/Fe prepared without TX-100. This also influenced the dechlorination pathway.

3.6. Successive reduction of HCB by different Cu/Fe reductants

The successive reduction of HCB by the three bimetal systems was studied to evaluate the long-term performance of the reductants. As shown in Fig. 7, after four cycles of successive supernatant replacement (12 h treatment), the reduction by Cu/Fe in aqueous TX-100 solution was still maintained at high level (above 98%), the reduction by Cu/Fe adsorbed with TX-100 was slightly decreased, and the reduction by Cu/Fe prepared with TX-100 was greatly reduced. It should be noted that the reduction herein denoted the change of HCB concentration in aqueous solution, instead of the total concentration given in former sections. In the successive replacement, Fe was increasingly consumed and TX-100 in Cu/Fe adsorbed and prepared was gradually released. Actually, significant reduce of iron quantity was apparently observed in the later cycles.

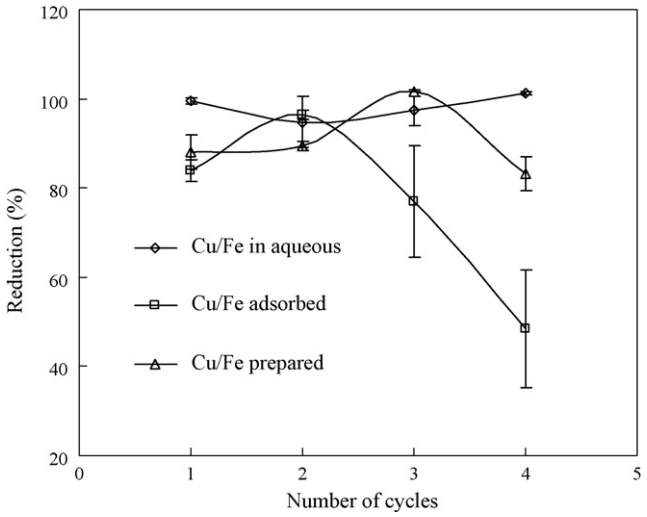

Fig. 7. Successive reduction of HCB by different Cu/Fe reductants.

However, the stable reduction efficiency with Cu/Fe in aqueous indicates that the loss of iron quantity during the four replacements had minute influence on the reduction. So, the continuous release of TX-100 was responsible for the decreased reduction. Although the desorption of TX-100 from Cu/Fe adsorbed and prepared was found to be minimal in Section 3.2, the desorption may become significant with the change of Cu/Fe surface after long time treatment. Park et al. [17] compared the successive reduction of octahydro-1,3,5,7-tetranitro-1,3,5,7-tetrazocine (HMX) by Fe particles in aqueous didecyldimethylammonium bromide (didecyl) solution and by Fe particles adsorbed with didecyl. It was also demonstrated that HMX reduction was maintained at high level by Fe in aqueous didecyl, but was gradually reduced by Fe adsorbed with didecyl.

4. Conclusions

This study investigated the catalytic reductive dechlorination of HCB by Cu/Fe influenced by TX-100. Different Cu/Fe reductants were prepared and characterized. The sorption/desorption kinetics and isotherm of TX-100 on Cu/Fe were also investigated. The main conclusions are drawn as follows.

(1) The reduction of HCB by Fe alone in the presence and absence of TX-100 was negligible even for a long time, the loading of Cu significantly enhanced the reduction. The reduction by Cu/Fe increased with the increase in TX-100 concentration in aqueous solution, reached the maximum of 96.8% when the aqueous TX-100 was around CMC, and decreased with the further increase in TX-100 concentration. The mechanism was suggested as the increased mass transport to reactive sites at low TX-100 concentration below CMC and the coverage of reactive sites at high TX-100 concentration above CMC.
(2) The greatest reduction was achieved by Cu/Fe in the presence of TX-100, followed by Cu/Fe adsorbed and prepared with TX-100. PeCB and TeCB were identified as the main dechlorination intermediates in the reduction by different Cu/Fe. The successive reduction could be maintained at high level by Cu/Fe in aqueous TX-100 solution, was slightly decreased by Cu/Fe adsorbed with TX-100, and was greatly reduced by Cu/Fe prepared with TX-100.
(3) Although Cu/Fe bimetal can dechlorinate HCB in aqueous solution and the presence of TX-100 shows enhancement, effort is still needed to reach a complete dechlorination. Our follow-

ing work will investigate the dechlorination by nanoscale Cu/Fe bimetal.

Acknowledgements

This work was supported by the International Foundation for Science (IFS, No. W/4500-1), Natural Science Foundation of China (NSFC, No. 20777024, No. 40801114), and the Open Fund of State Key Laboratory of Soil and Sustainable Agriculture (No. 0812000046). The Analytical and Testing Center of Huazhong University of Science and Technology is thanked for its help in reductant characterization.

References

[1] S.N. Meijer, W.A. Ockenden, A. Sweetman, K. Breivik, J.O. Grimalt, K.C. Jones, Global distribution and budget of PCBs and HCB in background surface soils: implications for sources and environmental processes, Environ. Sci. Technol. 37 (2003) 667–672.
[2] N.Q. Ren, M.X. Que, Y.F. Li, Y. Liu, X.N. Wan, D.D. Xu, E. Sverko, J.M. Ma, Polychlorinated biphenyls in Chinese surface soils, Environ. Sci. Technol. 41 (2007) 3871–3876.
[3] USEPA, Contaminated sediment remediation guidance for hazardous waste sites, 2005.
[4] S.H. Yuan, M. Tian, X.H. Lu, Electrokinetic movement of hexachlorobenzene in contaminated soils enhanced by Tween 80 and β-cyclodextrin, J. Hazard. Mater. B137 (2006) 1218–1225.
[5] L.J. Matheson, P.G. Tratnyek, Reductive dehalogenation of chlorinated methanes by iron metal, Environ. Sci. Technol. 28 (1994) 2045–2053.
[6] D.M. Cwiertny, S.J. Bransfielf, K.J.T. Livi, D.H. Fairbrother, A.L. Roberts, Exploring the influence of granular iron additives on 1,1,1-trichloroethane reduction, Environ. Sci. Technol. 40 (2006) 6837–6843.
[7] S.W. Jeen, K.U. Mayer, R.W. Gihham, D.W. Blowes, Reactive transport modeling of trichloroethene treatment with declining reactivity of iron, Environ. Sci. Technol. 41 (2007) 1432–1438.
[8] Y. Xu, W.X. Zhang, Subcolloidal Fe/Ag particles for reductive dehalogenation of chlorinated benzenes, Ind. Eng. Chem. Res. 39 (2000) 2238–2244.
[9] G.V. Lowry, K.M. Johnson, Congener-specific dechlorination of dissolved PCBs by microscale and nanoscale zerovalent iron in a water/methanol solution, Environ. Sci. Technol. 38 (2004) 5208–5216.
[10] C. Grittini, M. Malcomson, Q. Fernando, N. Korte, Rapid dechlorination of polychlorinated biphenyls on the surface of a Pd/Fe bimetallic system, Environ. Sci. Technol. 29 (1995) 2898–2900.
[11] C.B. Wang, W.X. Zhang, Synthesizing nanoscale iron particles for rapid and complete dechlorination of TCE and PCBs, Environ. Sci. Technol. 31 (1997) 2154–2156.
[12] F. He, D.Y. Zhao, Preparation and characterization of a new class of starch-stabilized bimetallic nanoparticles for degradation of chlorinated hydrocarbons in water, Environ. Sci. Technol. 39 (2005) 3314–3320.
[13] M.M. Scherer, K.M. Johnson, J.C. Westall, P.G. Tratnyek, Mass transport effects on the kinetics of nitrobenzene reduction by iron metal, Environ. Sci. Technol. 35 (2001) 2804–2811.
[14] G.D. Sayles, G. You, M. Wang, M.J. Kupferle, DDT, DDD, and DDE dechlorination by zero-valent iron, Environ. Sci. Technol. 31 (1997) 3448–3454.
[15] D.S. Alessi, Z. Li, Synergistic effect of cationic surfactants on perchloroethylene degradation by zero-valent iron, Environ. Sci. Technol. 35 (2001) 3713–3717.
[16] G.A. Loraine, Effects of alcohols, anionic and nonionic surfactants on the reduction of PCE and TCE by zero-valent iron, Water Res. 35 (2001) 1453–1460.
[17] J. Park, S.D. Comfort, P.J. Shea, J.S. Kim, Increasing Fe^0-mediated HMX destruction in highly contaminated soil with didecyldimethylammonium bromide surfactant, Environ. Sci. Technol. 39 (2005) 9683–9688.
[18] P. Zhang, H.K. Jones, P. Zhang, R.S. Bowman, Chromate transport through columns packed with surfactant-modified zeolite/zero valent iron pellets, Chemosphere 68 (2007) 1861–1866.
[19] H.H. Cho, J.W. Park, Sorption and reduction of tetrachloroethylene with zero valent iron and amphiphilic molecules, Chemosphere 64 (2006) 1047–1052.
[20] B.W. Zhu, T.T. Lim, J. Feng, Influences of amphiphiles on dechlorination of a trichlorobenzene by nanoscale Pd/Fe: adsorption, reaction kinetics, and interfacial interactions, Environ. Sci. Technol. 42 (2008) 4513–4519.
[21] S.J. Bransfield, D.M. Cwiertny, A.L. Roberts, D.H. Fairbrother, Influence of copper loading and surface coverage on the reactivity of granular iron toward 1,1,1-trichloroethane, Environ. Sci. Technol. 40 (2006) 1485–1490.
[22] L.R. Lu, Z.H. Ai, J.P. Li, Z. Zheng, Q. Li, L.Z. Zhang, Synthesis and characterization of $Fe–Fe_2O_3$ core-shell nanowires and nanonecklaces, Cryst. Growth Des. 7 (2007) 459–464.
[23] R.A. Doong, Y.L. Lai, Effect of metal ions and humic acid on the dechlorination of tetrachloroethylene by zerovalent iron, Chemoshpere 64 (2006) 371–378.
[24] J. Quinn, C. Geiger, C. Clausen, K. Brooks, C. Coon, S. O'Hara, T. Krug, D. Major, W.S. Yoon, A. Gavaskar, T. Holdsworth, Field demonstration of DNAPL dehalogenation using emulsified zero-valent iron, Environ. Sci. Technol. 39 (2005) 1309–1318.
[25] Y.H. Liou, S.L. Lo, C.J. Lin, C.Y. Hu, W.H. Kuan, S.C. Weng, Methods for accelerating nitrate reduction using zerovalent iron at near-neutral pH: effects of H_2-reducing pretreatment and copper deposition, Environ. Sci. Technol. 39 (2005) 9643–9648.
[26] A.B.M. Giasuddin, S.R. Kanel, H. Choi, Adsorption of humic acid onto nanoscale zerovalent iron and its effect on arsenic removal, Environ. Sci. Technol. 41 (2007) 2022–2027.
[27] Z.H. Li, C. Willms, J. Alley, P.F. Zhang, R.S. Bowman, A shift in pathway of iron-mediated perchloroethylene reduction in the presence of sorbed surfactant—a column study, Water Res. 40 (2006) 3811–3819.
[28] M.C. Lu, J. Anotai, C.H. Liao, W.P. Ting, Dechlorination of hexachlorobenzene by zero-valent iron, Pract. Period. Hazard. Toxic Radioact. Waste Manage. ASCE 8 (2004) 136–140.
[29] B.W. Zhu, T.T. Lim, J. Feng, Reductive dechlorination of 1,2,4-trichlorobenzene with palladized nanoscale Fe^0 particles supported on chitosan and silica, Chemosphere 65 (2006) 1137–1145.
[30] Y. Shih, Y. Chen, M. Chen, Y. Tai, C. Tso, Dechlorination of hexachlorobenzene by using nanoscale Fe and nanoscale Pd/Fe bimetallic particles, Colloid Surf. A: Physicochem. Eng. Aspects 332 (2009) 84–89.